doi:10.3772/j.issn.1006-6748.2019.04.012

Research on static bearing characteristics of magnetic-liquid double suspension bearing①

Zhao Jianhua(赵建华)*,**, Wang Qiang*, Zhang Bin*, Chen Tao*, Gao Dianrong②*
(*Hebei Provincial Key Laboratory of Heavy Machinery Fluid Power Transmission and Control, Yanshan University, Qinhuangdao 066004, P. R. China)
(**Jiangsu Provincial Key Laboratory of Advanced Manufacture and Process for Marine Mechanical Equipment, Zhenjiang 212003, P. R. China)

Abstract

Due to low viscosity of seawater, it is difficult to form a seawater-lubricated film. It is easy to cause the overload and burning phenomenon of seawater-lubrication sliding bearing, and then the operation stability and service life can be shortened seriously. Therefore, the paper introduces an electromagnetic suspension theory into the seawater lubricated sliding bearing. Then a novel magnetic-liquid double suspension bearing can be formed, which can enhance bearing capacity and stiffness greatly. Firstly, the structural characteristics, support-adjustment mechanism of magnetic-liquid double suspension bearing is analyzed. Secondly, based on force balance equation, electromagnetic equation and flow equation, the transfer functions of single DOF bearing system of magnetic-liquid double suspension bearing under constant-flow supply model are deduced. Then bearing capacity, static stiffness and total power loss are selected as static performance indexes. The influence rule of operaton and structural parameters on the static performance of single DOF bearing system will be analyzed. The results show that bearing capacity decreases with the increase of liquid film thickness and width of edge seals, bias current and coil turns decrease. Static stiffness decreases with the increase of liquid film thickness, edge seals width, bias current and coil turns. Total power loss decreases with the increase of liquid film thickness, edge seals width, bias current and coil turns decrease. And static performance indexes can not be affected by liquid viscosity. The proposed research provides some theoretical and experimental basis for the parameter design of magnetic-liquid double suspension bearing.

Key words: magnetic-liquid double suspension bearing, static performance index, bearing capacity, static stiffness, total power loss

0 Introduction

Due to the advantage of widespread sources, low price, non-pollution of seawater that can be recycled and so on, seawater lubricated bearing is widely used in engineering practice such as hydropower generation, deep-sea exploration and so on. However, due to the low viscosity, it is difficult to form lubricating film, and then the bearing capacity and stiffness of seawater lubricated film are very poor. It is easy to cause overload and burning phenomenon, and the operation stability and service life can be greatly shortened.

Magnetic bearings adopt a non-contact supporting structure, which has the advantages of no friction and wear, high precision, strong reliability, low energy consumption and no lubrication, etc. It is very suitable as an auxiliary supporting form for seawater lubrication bearing. Therefore, this work introduces magnetic suspension concept into hydrostatic bearing in order to form magnetic-liquid double suspension bearing, and it can further improve the bearing capacity and stiffness.

Due to combining the magnetic bearing and hydrostatic bearing together to form a new type of supporting system, the static performance such as bearing capacity, static stiffness and power loss on the bearing per-

① Support by the National Natural Science Foundation of China (No. 51705445), the Open Project Funding of Hebei Provincial Key Laboratory of Heavy Machinery Fluid Power Transmission and Control and the Open Project Funding of Jiangsu Provincial Key Laboratory of Advanced Manufacture and Process for Marine Mechanical Equipment.

② To whom correspondence should be addressed. E-mail: gaodr@ysu.edu.cn

Received on Nov. 8, 2018

formance of magnetic-liquid double suspension bearing needs to be further studied. This paper will analyze the force of magnetic-liquid double suspension bearing under a constant flow supply model. And according to the transfer function, the influence of different parameters (film thickness, bias current and electromagnetic coil turns etc.) on system static performance will be analyzed.

In recent years, many scholars have done deep research on hydrostatic bearing and electromagnetic bearing, and acquired large achievements. In Ref. [1], flexibility analysis of the rotor-AMBs system was carried out, and the dynamic equations of the rotor-AMBs system, critical speed, logarithmic attenuation rate and vibration modal shapes of the rotor were obtained. The bearing capacity and influencing factors of water-lubricated thrust bearing were analyzed. In Ref. [2], the results showed that the bearing capacity of the bearing could be improved by choosing appropriate friction pair and PV value. In Ref. [3], a 3-dimensional finite element model of bearing was formulated by Gambit and FLUENT simulation. And the results showed that oil film pressure peak value of the deep/shallow pockets hybrid bearing appeared in every shallow pocket, and the carrying capacity was increased with the increase of eccentricity and rotational speed. In Ref. [4], a single degree of freedom maglev double-closed-loop control system was established to analyze the influence of current inside loop on system response speed and stability. The results showed that the current feedback accelerated control system responds speed, which is beneficial to the system stability, and can improve dynamic stiffness and critical speed.

At present, hydrostatic-suspension and magnetic-suspension bearing system are studied separately by domestic and foreign scholars. But static bearing characteristics of magnetic-liquid double suspension bearing has not been reported. Static bearing characteristics are the basis for analyzing the running stability and service life of magnetic-liquid double suspension bearing[5-8].

Therefore, static bearing characteristics of magnetic-liquid double suspension bearing are analyzed in the paper. The research of the paper provides the theoretical basis for designing magnetic-liquid double suspension bearing.

1 Introduction of magnetic-liquid double suspension bearing

Magnetic-liquid double suspension bearing system with seawater lubricated is mainly composed of base, shell, flux sleeve (cold-rolled, non-oriented silicon-steel and galvanized), coil turns, stator (electric iron + galvanized), rotor and other components, as shown in Fig. 1 and Fig. 2. Eight NSSNNSSN magnetic poles are distributed along the circumferential direction. Two adjacent heteropolar magnetic poles pairs are formed into one magnetic-pole-pair. And a magnetic circuit between magnetic-pole-pair and flux sleeve will be formed to produce electromagnetism. Each pole pair has a liquid inlet hole in supporting cavity. When seawater through the gap between magnetic pole and flux sleeve, then the hydrostatic bearing force can be generated.

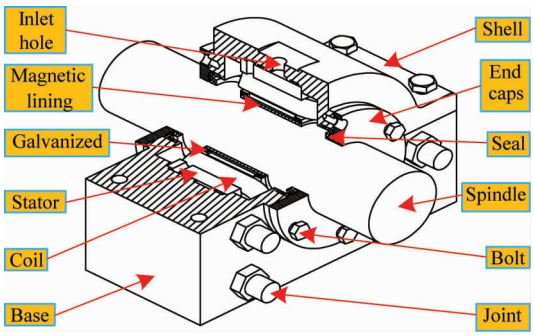

Fig. 1 Semi-isometric view of magnetic-liquid double suspension bearing

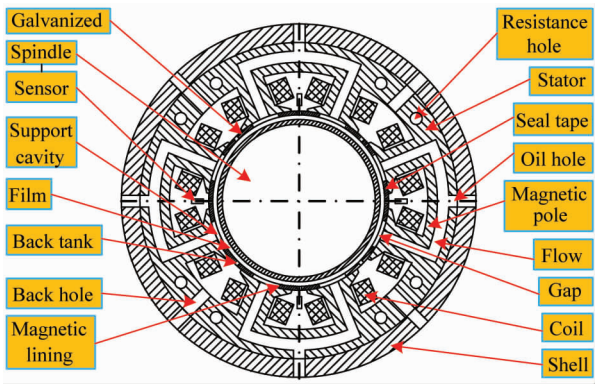

Fig. 2 Full-sections drawing of magnetic-liquid double suspension bearing

Magnetic-liquid double suspension bearing system includes magnetic suspension and hydrostatic suspension support system (adjustment principle can be shown in Fig. 3). The additional electromagnetic force can be introduced into the magnetic-liquid double suspension bearing system, and double support of electromagnetic force and hydrostatic force in real time can be achieved. So that bearing capacity, stiffness and operational stability can be significantly increased, and the service life is prolonged. And then magnetic-liquid double suspension bearing system is very suitable for low-speed, over-loaded and frequent-start occasion.

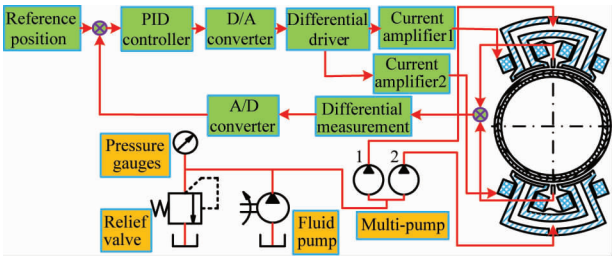

Fig. 3 Single degree freedom support regulation principle of magnetic-liquid double suspension bearing

Eight magnetic poles are evenly distributed along circumference. Two adjacent heteropolar magnetic poles pairs are formed into one magnetic-pole-pair. In initial state, electromagnetic force and hydrostatic force of 2 adjacent heteropolar magnetic poles of magnetic pole pair are separately equal. So magnetic pole pair is analyzed as a unit, and then it can be called as support unit (force analysis as shown in Fig. 4).

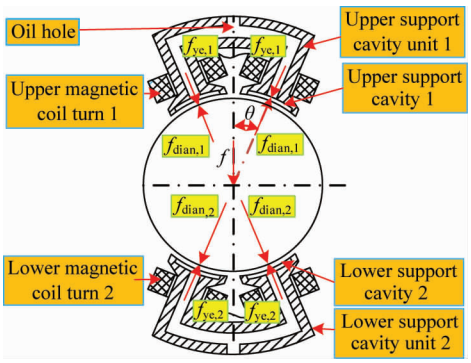

Fig. 4 Force diagram of single degree freedom magnetic-liquid double suspension bearing

Under the external load, the parameters of PID controller are adjusted, and electromagnetic force and hydrostatic force can be adjusted in certain proportion in real time to support the external load (as shown in Fig. 5).

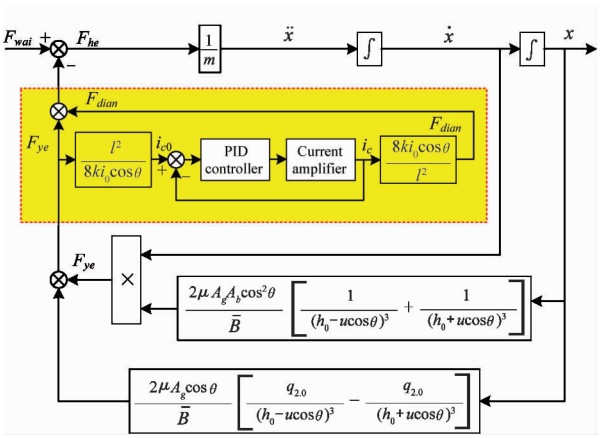

Fig. 5 Control block diagram of magnetic-liquid double suspension bearing

2 Transfer function of single DOF bearing system

In order to study the bearing characteristics of magnetic-liquid double suspension bearing, the following assumptions are made[8-10]:

1) Flow status of lubricant liquid is laminar flow, and inertial force is ignored.

2) Due to low pressure, pressure-viscosity character is ignored.

3) MFL is ignored, and flux is uniformly distributed in magnetic circuit.

4) Reluctance of core and rotor are ignored, and magnetic potential only acts on the air.

5) Magnetic hysteresis and eddy current effects are ignored.

6) Supporting surface is assumed to be rigid body.

2.1 Initial state of a single DOF system

Take single DOF system as the research object, which consists of upper and lower support unit (it is shown in Fig. 3 and Fig. 4). Single DOF system adopts the control way of overall open-loop and local closed-loop[11] (it is shown in Fig. 5).

In initial state, liquid film thickness, bias current, and electromagnetic force of upper and lower support unit are separately equal, and gravity of rotor can be neglected.

1) Current equation current amplifier is used in the magnetic-liquid double suspension bearing system. And the bias current of the initial state is shown as follows:

$$i_{pian,1,0} = i_{pian,2,0} = i_0 \tag{1}$$

where $i_{pian,1,0}$ is current of upper magnetic 1 (A), $i_{pian,2,0}$ is current of lower magnetic 2 (A). i_0 is current of current amplifier (A).

2) Flow equation magnetic-liquid double suspension bearing adopts constant-flow supply mode, and flow equation of the upper and lower support cavity 1and 2 can be shown as follows[12-13,16]:

$$\begin{cases} q_{1,0} = q_{fa,1,0} \\ q_{2,0} = q_{fa,2,0} \end{cases} \tag{2}$$

where $q_{1,0}$ is initial flow of upper support cavity 1 (L/min), $q_{2,0}$ is initial flow of lower support cavity 2 (L/min), $q_{fa,1,0}$ is initial flow of multi-pump outlet 1 (L/min), $q_{fa,2,0}$ is initial flow of multi-pump outlet 2 (L/min).

3) Hydrostatic force according to Navier-Stokes equation, hydrostatic force ($f_{ye,1,0}$ and $f_{ye,2,0}$) of upper and lower cavity 1 and 2 are shown as follows:

$$\begin{cases} f_{ye,1,0} = 2p_{1,0}A_e\cos\theta = 2q_{1,0}R_0A_e\cos\theta \\ f_{ye,2,0} = 2p_{2,0}A_e\cos\theta = 2q_{2,0}R_0A_e\cos\theta \end{cases} \quad (3)$$

where, θ is angle between centerline of support cavity and plumb line (as shown in Fig. 3 and Fig. 4) (°), $p_{1,0}$ is pressure of upper support cavity 1 (MPa), $p_{2,0}$ is pressure of lower support cavity 2 (MPa). μ is dynamic viscosity of seawater (Pa · s), R_0 is liquid resistance of upper and lower support cavity 1, 2 (N · s/m^5).

$$R_0 = \frac{\mu}{\bar{B}h_0^3}$$

where $\bar{B}$ is flow coefficient of support cavity (dimensionless).

$$\bar{B} = \frac{A-a}{6b} + \frac{B-b}{6a}$$

where A_e is bearing area of support cavity (m^2).

$$A_e = (A-a)(B-b)$$

where A is length of support cavity along axial direction (m) (as shown in Fig. 6). B is width of support cavity along circumferential direction (m) (as shown in Fig. 6). a is sealing tape width of support cavity along axial direction (m) (as shown in Fig. 6). b is sealing tape width of support cavity along circumferential direction (m) (as shown in Fig. 6).

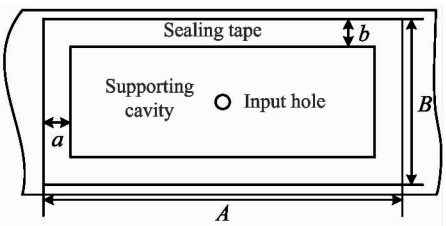

Fig. 6 Structure of support cavity

4) Electromagnetic force according to Maxwell attractive formula, $f_{dian,1,0}$, $f_{dian,2,0}$ can be shown as follows:

$$f_{dian,1,0} = f_{dian,2,0} = 2k\frac{i_0^2}{(h_0+l)^2}\cos\theta \quad (4)$$

where k is electromagnetic coefficient (H · m), $k = \frac{\mu_0 N^2 A_1}{4}$; h_0 is initial liquid film thickness (m). l is thickness of zinc coating (m); μ_0 is permeability of air (H/m), $\mu_0 = 4\pi \times 10^{-7}$; N is coil turns (dimensionless); A_1 is area of core (m^2) (as shown in Fig. 5). $A_1 = AB$

5) Mechanical balance equation of rotor based on Newton's second law, mechanical balance equation of rotor is obtained as follows:

$$f_{dian,1,0} + f_{ye,2,0} - f_{dian,2,0} - f_{ye,1,0} = mg \quad (5)$$

where m is mass of rotor (kg), g is gravity acceleration (m/s^2).

2.2 Working state of single DOF system

Under the external load, the displacement of rotor is x, and the liquid film thickness of upper and lower support cavity h_1, h_2 are shown as follows[14-16]:

$$\begin{cases} h_1 = h_0 + x\cos\theta \\ h_2 = h_0 - x\cos\theta \end{cases} \quad (6)$$

1) Current equation, during the process of applying external load, the control current of bearing system and electromagnetic force are changed. So the output current of the current amplifier is

$$i_{pian,1,1} = i_{pian,2,1} = i_0 + i_c \quad (7)$$

where $i_{pian,1,1}$ is current of upper magnetic 1 (A), $i_{pian,2,1}$ is current of upper magnetic 2 (A), i_c is control current (A).

2) Flow equation, when the film thickness changes, the liquid resistance of upper and lower support cavity changes. At the same time, considering the influence of the sensitive oil volume, the flow rate of the upper and lower support cavity is shown as follows:

$$\begin{cases} q_1 = q_{fa,1,0} - A_b\dot{h}_1 - \frac{V_{oa}}{E}\dot{p}_1 \\ q_2 = q_{fa,2,0} - A_b\dot{h}_2 - \frac{V_{oa}}{E}\dot{p}_2 \end{cases} \quad (8)$$

where q_1 is flow of upper support cavity 1 (L/min), q_2 is flow of lower support cavity 2 (L/min), A_b is equivalent extrusion area of support cavity (m^2) $A_b = (A-2a)(B-2b)$, V_{oa} is volume of sensitive liquid path, between multi-pump and support cavity (m^3), E is elastic modulus of seawater (MPa), p_1 is pressure of upper support cavity 1 (MPa), p_2 is pressure of lower support cavity 2 (MPa).

3) Hydrostatic force similarly, hydrostatic force $f_{ye,1}$, $f_{ye,2}$) of upper and lower support cavity 1, 2 is shown as follows:

$$\begin{cases} f_{ye,1} = 2q_1R_1A_e\cos\theta \\ f_{ye,2} = 2q_2R_2A_e\cos\theta \end{cases} \quad (9)$$

where R_1 is liquid resistance of upper support cavity 1 (N · s/m^5), $R_1 = \frac{\mu}{\bar{B}h_1^3}$; R_2 is liquid resistance of lower support cavity 2 (N · s/m^5), $R_2 = \frac{\mu}{\bar{B}h_2^3}$.

4) Electromagnetic force similarly, the electromagnetic force ($f_{dian,1}$, $f_{dian,2}$) of upper and lower poles 1, 2 is shown as follows:

$$\begin{cases} f_{dian,1} = 2k\frac{(i_0+i_c)^2}{(h_1+l)^2}\cos\theta \\ f_{dian,2} = 2k\frac{(i_0-i_c)^2}{(h_2+l)^2}\cos\theta \end{cases} \quad (10)$$

where i_c is control current (A), h_1 is upper support

cavity liquid film thickness (m), h_2 is lower support cavity liquid film thickness (m).

As the entire bearing system is regulated to PID controller, and electromagnetic force and hydrostatic force in a certain proportion collectively bear external load. Set the proportion coefficient be λ. Under the external load a proportional change is producted which is shown as follows:

$$\Delta f_{ye} = \lambda \Delta f_{dian} \tag{11}$$

where, $\Delta f_{ye} = f_{ye,2} - f_{ye,1}$, $\Delta f_{dian} = f_{dian,1} - f_{dian,2}$, $\lambda = 1$.

According to Eq. (11), control current i_c can be obtained as follows:

$$i_c = \frac{(q_2 R_2 - q_1 R_1) A_e (l + h_0)^2}{4 k i_0} \tag{12}$$

Based on Fig. 5, Eq. (11) can be expressed in the following form:

$$\Delta f_{dian} = \frac{k_p + \dfrac{k_i}{s} + k_d s}{1 + k_p + \dfrac{k_i}{s} + k_d s} \Delta f_{ye} \tag{13}$$

5) Mechanical balance equation of rotor similarly, mechanical balance equation of rotor is shown as follows:

$$f_{dian,1} + f_{ye,2} - f_{dian,2} - f_{ye,1} - f = -m\ddot{x} \tag{14}$$

where f is external load of rotor (N).

According to Eq. (1) – Eq. (14), and ignoring sensitive path volume V_{oa}, electromagnetic force and hydrostatic force are regulated by PID controller to maintain a certain proportion in real-time. Adjustment process is very short, and the response is very fast. Therefore, in order to simplify the calculation process, the electromagnetic force can be converted into hydrostatic force with a certain proportion in the process of static feature analysis, and the dynamic characteristics of bearing system are not affected. And external load f and displacement x of rotor can be considered as input and output criteria separately, and the transfer function of bearing system can be obtained as follows:

$$\begin{aligned} G(s) &= \frac{\Delta X(s)}{\Delta F(s)} \\ &= \frac{TT_3 s^3 + TT_2 s^2 + TT_1 s + TT_0}{\Gamma_5 s^5 + \Gamma_4 s^4 + \Gamma_3 s^3 + \Gamma_2 s^2 + \Gamma_1 s + \Gamma_0} \end{aligned} \tag{15}$$

The expression of TT_3, TT_2, TT_1, TT_0, Γ_5, Γ_4, Γ_3, Γ_2, Γ_1, Γ_0 as shown in Table 1.

Table 1 Schedule

Coefficients	Numerical value
TT_3	$\dfrac{A_b}{h_0^3} k_d$
TT_2	$\dfrac{A_b}{h_0^3}(1 + k_p) + \dfrac{3q_0}{h_0^4} k_d$
TT_1	$\dfrac{A_b}{h_0^3} k_i + \dfrac{3q_0}{h_0^4}(1 + k_p)$
TT_0	$k_i \dfrac{3q_0}{h_0^4}$
Γ_5	$\dfrac{A_b}{h_0^3} k_d m$
Γ_4	$\left[\dfrac{A_b}{h_0^3}(1 + k_p) + \dfrac{3q_0}{h_0^4} k_d\right] m + k_d \dfrac{A_b^2}{h_0^6} \dfrac{8\mu A_e \cos^2\theta}{\bar{B}}$
Γ_3	$\left[\dfrac{A_b}{h_0^3} k_i + \dfrac{3q_0}{h_0^4}(1 + k_p)\right] m + \left[\dfrac{A_b}{h_0^3}(1 + 2k_p) + \dfrac{12q_0}{h_0^4} k_d\right] \dfrac{4\mu A_e \cos^2\theta}{\bar{B}} \dfrac{A_b}{h_0^3}$
Γ_2	$k_i \dfrac{3q_0}{h_0^4} m + \left[k_i \dfrac{A_b^2}{h_0^6} + k_d \dfrac{9q_0^2}{h_0^8} + \dfrac{3A_b q_0}{h_0^7}(1 + 2k_p)\right] \dfrac{8\mu A_e \cos^2\theta}{\bar{B}}$
Γ_1	$12 \dfrac{q_0}{h_0^4} \dfrac{\mu A_e \cos^2\theta}{\bar{B}} \left(4k_i \dfrac{A_b}{h_0^3} + \dfrac{3q_0}{h_0^4}(1 + 2k_p)\right)$
Γ_0	$k_i \dfrac{72\mu A_e \cos^2\theta}{\bar{B}} \dfrac{q_0^2}{h_0^8}$

When $k_p = 1$, $k_d = 0$, $k_i = 0$, the transfer function can be reduced as follows:

$$\frac{\Delta X(s)}{\Delta F(s)} = \frac{1}{T_2 s^2 + T_1 s + T_0} \tag{16}$$

where, $T_2 = m$, $T_1 = \dfrac{6\mu A_e A_b \cos^2\theta}{\bar{B} h_0^3}$, $T_0 = \dfrac{18\mu q_0 A_e \cos^2\theta}{\bar{B} h_0^4}$.

3 Static performance of single DOF supporting unit

3.1 Static performance indexes

Static performance indexes mainly include carrying capacity F_0, static stiffness j_0 and total power loss W_{zong}.

1) Carrying capacity F_0. When the rotor displacement reaches its maximum value, and the external load f reaches the limit value, it is called carrying capacity F_0. The expression of carrying capacity F_0 is shown as follows:

$$F_0 = 2\cos\theta \sum_{i=1}^{2} \left\{ (-1)^i p_{i,1} A_e - \frac{k[i_0 - (-1)^i i_c]^2}{(h_{i,1} + l)^2} \right\} \tag{17}$$

2) Static stiffness j_0. It represents the ability of liquid film to resist deformation caused by external load. The expression of static stiffness j_0 is shown as follows:

$$j_0 = -\frac{\partial F}{\partial h} = 2\cos\theta \left\{ \sum_{i=1}^{2} \frac{2k[i_0 - (-1)^i i_c]^2}{(h_{i,1} + l)^3} + \frac{3\mu q_{i,1} A_e}{\bar{B} h_{i,1}^4} \right\} \tag{18}$$

3) Total power loss W_{zong}. Total power loss is the sum of support cavity power loss and electromagnetic coil heat loss, which is shown as follows:

$$W_{zong} = \frac{4\mu A_s A_e}{A_t} \left(\sum_{i=1}^{2} \frac{q_i}{h_i} \right) + 2(i_0 + i_c)^2 R_{quan} + 2(i_0 - i_c)^2 R_{quan} \tag{19}$$

According to mathematical expression of static performance indexes, the parameters which can affect the static characteristics are shown as follows: film thickness, bias current, coil turns, sealing tape width and so on.

3.2 Magnetic-liquid double suspension bearing parameters

The design parameters of magnetic-liquid double suspension bearing are shown in Table 2.

Table 2 Design parameters of magnetic-liquid double suspension bearing

Rotor mess m(kg)	Dynamic viscosity μ(Pa·s)	Elastic modulus E(MPa)
66.82	1.3077×10^{-3}	2.4×10^3
Pole area A(mm^2)	Film thickness h_0(μm)	Zinc coating thickness l(mm)
1000	10	0.5
Coil number N(dimension-less)	Liquid cavity width A(m)	Liquid cavity length B(m)
633	0.1	0.02
Axial fluid sealing tape width b(m)	Surrounding fluid sealing tape width a(m)	Pump pressure ps(MPa)
0.004	0.006	3
Fluid cavity 1 pressure p_1(MPa)	Fluid cavity 2 pressure p_2(MPa)	Bias current size i_0(A)
1	1.3	1.2
Load f(N)	Load frequency w(Hz)	
2000	50	

3.3 Influence of parameters on static performance of magnetic-liquid double suspension bearing

From Eq. (17), Eq. (18), as film thickness increases, liquid resistance of support cavity decreases, and then bearing capacity F_0 and static stiffness j_0 decrease monotonously, and power loss W_{zong} increases, as shown in Fig. 7 – Fig. 9. But deceasing trend of bearing capacity becomes insignificant gradually and it can be ignored.

From Eq. (17), Eq. (18), in the initial state, ignoring the gravity, electromagnetic force and hydrostatic force in a certain proportion can bear external load.

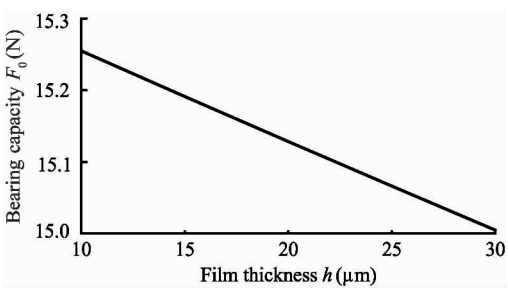

Fig. 7 Relationship between bearing capacity and liquid film thickness

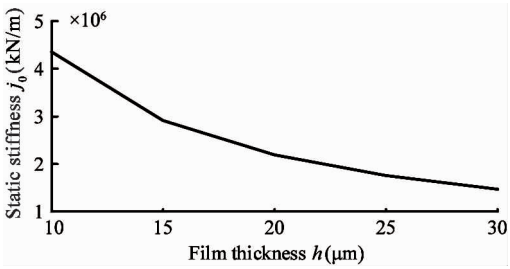

Fig. 8 Relationship between static stiffness and liquid film thickness

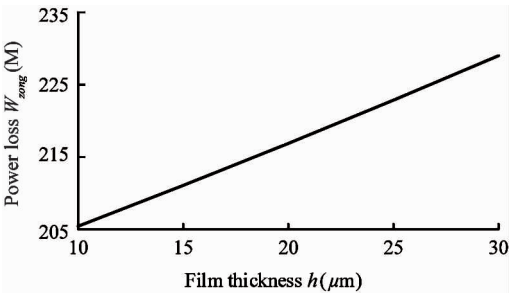

Fig. 9 Relationship between total power loss and liquid film thickness

Without control current, bias current makes less impact on electromagnetic force. As bias current increases gradually, bearing capacity F_0 increases and static stiffness j_0 decreases gradually, but the deceasing trend becomes insignificant gradually because electromagnetic parameters make less impact on bearing performance, and can be ignored. Power loss W_{zong} also decreases with the increase of bias current, as shown in Fig. 10 – Fig. 12.

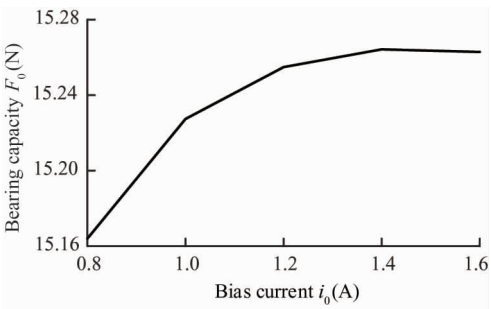

Fig. 10 Relationship between bearing capacity and bias current

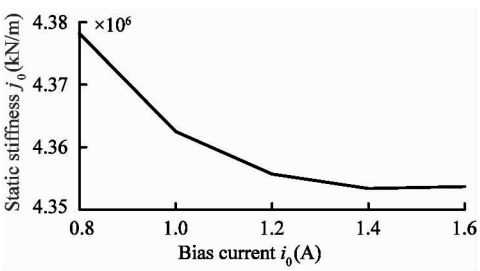

Fig. 11 Relationship between static stiffness and bias current

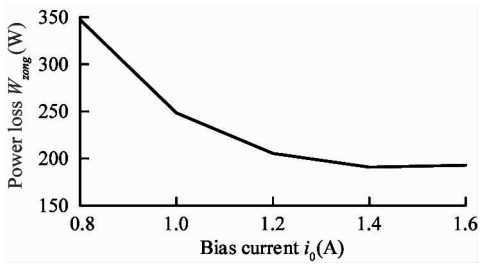

Fig. 12 Relationship between total power loss and bias current

From Eq. (17), Eq. (18), under the constant flow supply mode, the effective contact area between rotor and sealing tape is reduced with the increase of sealing tape width. And bearing capacity F_0, static stiffness j_0 and power loss W_{zong} are decreased with the increase of sealing tape width, as shown in Fig. 13 – Fig. 15.

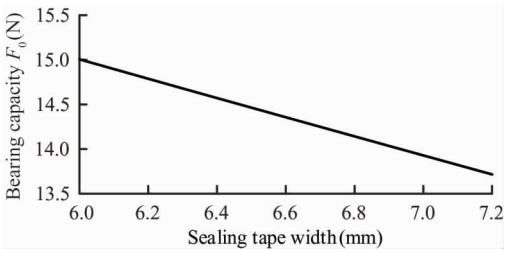

Fig. 13 Relationship between bearing capacity and sealing tape width

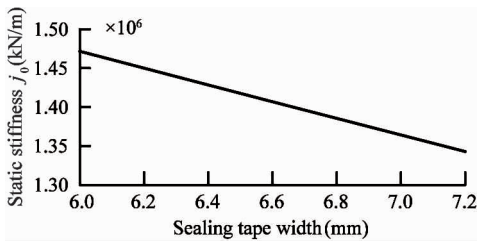

Fig. 14 Relationship between static stiffness and sealing tape width

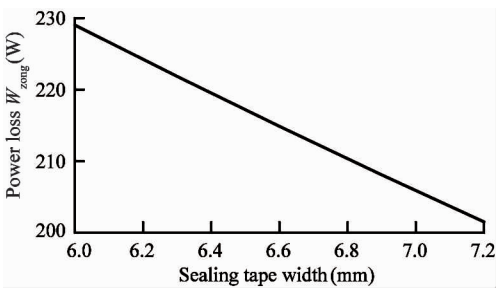

Fig. 15 Relationship between total power loss and sealing tape width

From Eq. (17), Eq. (18), with the increase of number of coil turns, coefficient of electromagnetic force k increases and electromagnetic force increases.

Because the electromagnetic force and the hydrostatic force collectively bear external load in a certain proportion, the hydrostatic force increases with the increase of electromagnetic force. Since the electromagnetic parameters make less impact on bearing performance, the deceasing trend of bearing capacity F_0, static stiffness j_0 become insignificant and can be ignored. Meanwhile power loss W_{zong} also decreases, as shown in Fig. 16 – Fig. 18.

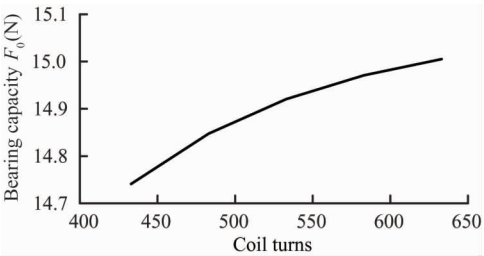

Fig. 16 Relationship between bearing capacity and coil turns

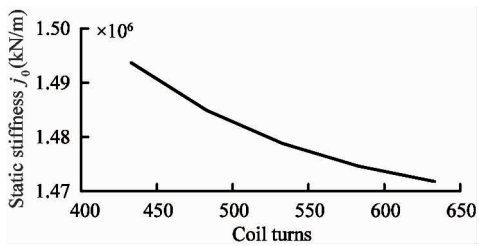

Fig. 17 Relationship between static stiffness and coil turns

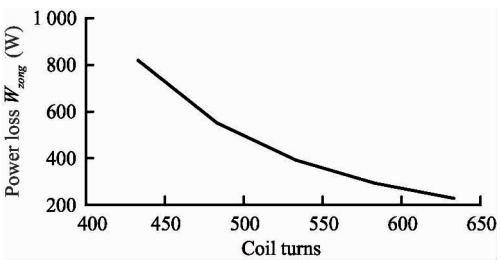

Fig. 18 Relationship between total power loss and coil turns

From Table 3, Eq. (17) and Eq. (18), it can be seen that with temperature rising, seawater viscosity almost keeps the same. So with the liquid viscosity increasing, the bearing capacity F_0, static stiffness j_0, and power loss W_{zong} are changed slightly, almost remain the same, as shown in Fig. 19 – Fig. 21.

Table 3 Dynamic viscosity of seawater (mPa · s)

Viscosity \ Temperature	10℃	20℃	30℃	40℃	50℃
	1.3077	1.0050	0.8007	0.6560	0.5494

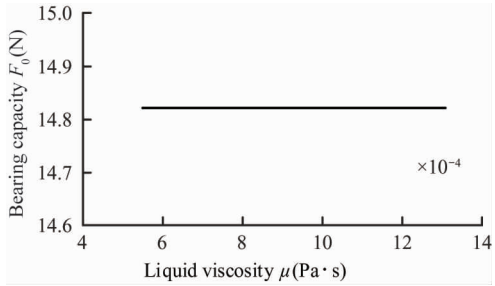

Fig. 19 Relationship between bearing capacity and liquid viscosity

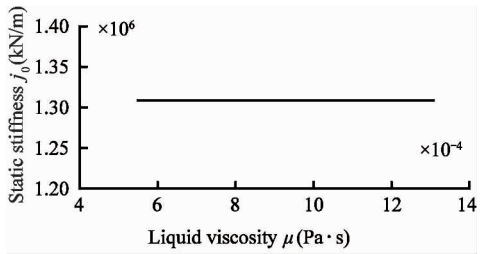

Fig. 20 Relationship between static stiffness and liquid viscosity

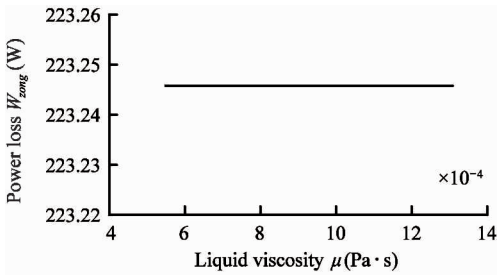

Fig. 21 Relationship between total power loss and liquid viscosity

4 Conclusion

With film thickness increasing and static stiffness j_0 decreasing, power loss W_{zong} increases, and bearing capacity F_0 can be ignored.

When the bias current increases gradually, bearing capacity F_0 and static stiffness j_0 almost remain the same, and power loss W_{zong} decreases.

With the sealing tape width increasing, bearing capacity F_0, static stiffness j_0 and power loss W_{zong} are decreased.

With increase of the number of coil turns, bearing capacity F_0 and static stiffness j_0 almost remain the same. Meanwhile the power loss W_{zong} decreases.

With the liquid viscosity increasing, bearing capacity F_0, static stiffness j_0, and power loss W_{zong} are changed slightly, almost remain the same.

Reference

[1] Liu N, Zhang G, Chen C J. Dynamic analysis on rotor

system supported by active electromagnetic bearings[J]. *Bearing*, 2006(8):5-7

[2] Zhang X, Zhou Y, Wang X R, et al. Research the influences on load capacity of water-lubricated thrust bearing [J]. *Machinery*, 2011, 49(4):16-19

[3] Liu H J, Guo H, Zhang S L. Research on static characteristics of deep/shallow pockets hybrid bearing based on FLUENT[J]. *Lubrication Engineering*, 2013, 38(10): 35-38

[4] Zhang W W, Hu Y F. Application of current feedback in magnetic bearing control[J]. *Machine Tool and Hydraulics*, 1999(4):44-44

[5] Cheng F, Ji W X. Simultaneous identification of bearing dynamic coefficients in a water-gas lubricated hydrostatic spindle with a big thrust disc[J]. *Journal of Mechanical Science and Technology*, 2016, 30(9):4095-4107

[6] Ginzburg B M, Bakhareva V E, Anisimov A V, et al. Polymeric materials for water-lubricated plain bearings [J]. *Russian Journal of Applied Chemistry*, 2006, 79 (5):695

[7] Jiang X P, Shi W D, Li W, et al. Rotor dynamic characteristics of water lubricated bearing for pumps[J]. *Transactions of the Chinese Society for Agricultural Machinery*, 2013, 44(1):62-66

[8] Zhao J H, Gao D R, Zhang Z C, et al. Indeterminate mechanics model of bearing capacity of constant pressure oil pockets in hydrostatic slide[J]. *Chinese Journal of Mechanical Engineering*, 2012, 48(22): 167-176 (In Chinese)

[9] Tu L, Li D M, Duan Z H. Pressure field numerical simulation of hydrodynamic bearing based on FLUENT[J]. *Lubrication Engineering*, 2011, 36(4):82-86

[10] Zhao J H, Zhou S L, Lu X H, et al. Numerical simulation and experimental study of heat-fluid-solid coupling of double flapper-nozzle servo valve[J]. *Chinese Journal of Mechanical Engineering*, 2015, 28(5): 1030-1038

[11] Kong X D, Wang Y Q. Control Engineering Fundamentals[M]. Beijing: China Machine Press, 2007: 12-15

[12] Wang X, Yamaguchi A. Characteristics of hydrostatic bearing/seal parts for water hydraulic pumps and motors. Part 1: experiment and theory[J]. *Tribology International*, 2002, (35): 425-433

[13] Zhao J H. The Oretical Analysis and Experimental Research of Liquid Hydrostatic Slide's Performance of Gantry Turning and Milling Center[D]. Hebei: Yanshan University, 2013: 15-20

[14] Ding Z Q. Design of Liquid Hydrostatic Bearing[M]. Shanghai: Shanghai scientific and Technical Publishers, 1989: 28-30

[15] Narita K, Priest M. Boundary Lubrication Film Formation From Belt Type CVT Fluids[M]. Essex: Woodhead Publishing, 2006: 39-50

[16] Zhao J H, Liang Y N, Gao D R. Oil pocket's bearing capacity analysis of liquid hydrostatic worktable in gentry moving milling center[J]. *Chinese Journal of Mechanical Engineering*, 2014, 27(5): 1008-1017

Zhao Jianhua, born in 1983. He received his Ph. D degree from Yanshan University in 2013. He also received his B. S. and M. S. degrees from Yanshan University in 2006 and 2010 respectively. Now, he is an associate professor in School of Mechanical Engineering, Yanshan University, P. R. China. His research interests include the simulation and analysis of hydrostatic bearing.